

Spatiotemporal evolution in a (2+1)-dimensional chemotaxis model

S. Banerjee^{a,*}, A. P. Misra^{b,1}, L. Rondoni^{a,c}

^aDipartimento di Matematica, Politecnico di Torino, Corso Duca degli Abruzzi 24, 10129 Torino, Italy

^bDepartment of Physics, Umeå University, SE-901 87 Umeå, Sweden

^cINFN, Sezione di Torino, Via P. Giuria 1, 10125 Torino, Italy

Abstract

Simulations are performed to investigate the nonlinear dynamics of a (2+1)-dimensional chemotaxis model of Keller-Segel (KS) type with a logistic growth term. Because of its ability to display auto-aggregation, the KS model has been widely used to simulate self-organization in many biological systems. We show that the corresponding dynamics may lead to a steady-state, divergence in a finite time as well as the formation of spatiotemporal irregular patterns. The latter, in particular, appear to be chaotic in part of the range of bounded solutions, as demonstrated by the analysis of wavelet power spectra. Steady states are achieved with sufficiently large values of the chemotactic coefficient (χ) and/or with growth rates r below a critical value r_c . For $r > r_c$, the solutions of the differential equations of the model diverge in a finite time. We also report on the pattern formation regime for different values of χ , r and the diffusion coefficient D .

Keywords: Spatiotemporal chaos, Chemotaxis model, pattern formation, wavelet spectrum

1. Introduction

The Keller and Segel (KS) model [1] is one of the most extensively studied chemotaxis models; it describes, for instance, the aggregation of cellular slime molds driven by chemical attraction. Because it gives rise to “auto-aggregation”, the KS model is used to describe many other phenomena including astrophysical ones [2, 3, 4]. Its mathematical properties, such as the existence of global solutions in time for certain choices of parameters and the finite time divergence for other choices, are understood to some extent [5, 6, 7]. In particular, it is known that solutions of the one-dimensional case may diverge in a finite time only if the chemoattractant does not diffuse, but in higher dimensional spaces divergences are common [7]. Also, Painter *et al* have shown that the KS model allows pattern formation and spatiotemporal chaos in one spatial dimension [6], but these features have not been investigated in full detail in the (2+1)-dimensional case.

Therefore, in this paper, we consider the (2+1)-dimensional KS model with a logistic growth term, which in dimensionless form reads [5, 6]:

$$\frac{\partial u}{\partial t} = \nabla \cdot (D \nabla u - \chi u \nabla v) + ru(1 - u), \quad (1)$$

$$\frac{\partial v}{\partial t} = \nabla^2 v + u - v, \quad (2)$$

where $u(x, y, t)$ denotes the organism density and $v(x, y, t)$ describes the concentration of the chemical signal around the point (x, y) at time t . The coefficients D and χ respectively stand for the organism diffusion or motility and the chemotactic sensitivity. The validity of Eqs. (1) and (2) in the framework of chemotaxis is supported by some experiments on the *Escherichia coli* (*E.coli*) bacterium (see, e.g. Refs. [8, 9]) even if this model does not seem to reproduce all the observed chemotactic motions [8].

It is known that the solutions of Eqs. (1) and (2) with certain parameter choices reproduce an aggregation phenomenon which mimics chemotactic migration along the directions of gradients of self-produced chemicals. It remains to explore other regions of the parameters space in search of the parameter values which lead to globally existing solutions, the finite time divergence as well as the formation of regular patterns. Furthermore, it is interesting to know whether chaotic patterns arise in regions of bounded solutions.

In the present work, we investigate these questions by means of numerical simulations, and we show that the solutions of the KS equations in (2+1)-dimensions, with a logistic growth term, diverge in a finite time when the cellular growth rate r exceeds a critical value r_c .

A detailed discussion of different versions of the KS model and its applications to chemotaxis can be found in the literature, e.g., in Refs. [5, 6, 7, 10, 11, 12]. Chemotaxis is a biological process by which organisms alter their movements or orientations in response to chemical gradients and concerns, e.g., the behaviors of *E.Coli*, amoebae, endothelial and neutrophil cells. Furthermore, it is of interest in phenomena such as cancer cell metastasis, embryogenesis, angiogenesis, tissue homeostasis, wound healing, immune response, progression of

*Corresponding author.

Email addresses: santo.banerjee@polito.it (S. Banerjee),
apmisra@visva-bharati.ac.in (A. P. Misra),
lamberto.rondoni@polito.it (L. Rondoni)

¹Permanent address: Department of Mathematics, Visva-Bharati University, Santiniketan-731 235, India.

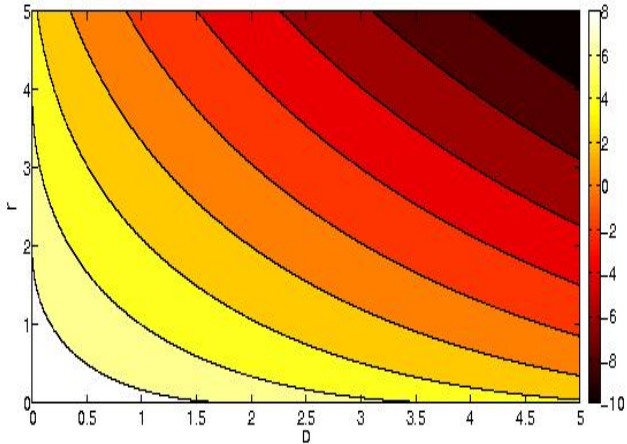


Figure 1: (Color online) The instability regions satisfying $\chi > (\sqrt{D} + \sqrt{r})^2$ (positive values in the colorbar) are shown in the (D, r) -plane.

diseases, finding food, forming the multicellular body of protozoa etc. [13, 14, 15]. In brief, chemotaxis is the process by which many organisms probe their environment and determine their movements in response to what they have found.

2. Nonlinear evolution

Equations (1) and (2) have a nontrivial steady-state solution $(u, v) = (1, 1)$. A linear stability analysis [6] through which different parameter regimes can be found for the formation of spatiotemporal patterns shows that the corresponding modes are unstable for $\chi > (\sqrt{D} + \sqrt{r})^2$ with wave numbers satisfying $k_1 < k < k_2$ where

$$k_{1,2}^2 = \frac{\chi - D - r}{2D} \mp \frac{1}{2D} \sqrt{(D + r - \chi)^2 - 4Dr}. \quad (3)$$

Thus, given a value of χ , the stable (negative values) and the unstable (positive values) regions can be represented in the (D, r) plane as in Fig. 1. In an interval $[0, L]$ with homogeneous Neumann (zero-flux) boundary conditions we have $k = n\pi/L$ with $n = 0, 1, 2, \dots$, whilst for periodic boundary conditions we have $k = 2n\pi/L$. We numerically investigate Eqs. (1) and (2) using zero-flux boundary conditions and with a time step $dt = 0.001$, grid size 200×200 in a simulation box of size $L_x \times L_y$ where $L_x = L_y = n\pi/k$. We explore the evolution of the density u and of the chemical concentration v in a larger domain, with an initial condition $(u, v) = (1, 1 + f(\epsilon))$, where $f(\epsilon) \lesssim 0.01$ is a spatially varying random perturbation. Furthermore, we perform a wavelet analysis of spectra to show that chaotic patterns may form in some parameter region corresponding to bounded solutions. This is important for the excitation of many modes in the nonlinear dynamics.

We note that for zero-flux boundary conditions on an interval of length L_x or L_y , the smallest non-vanishing mode is the

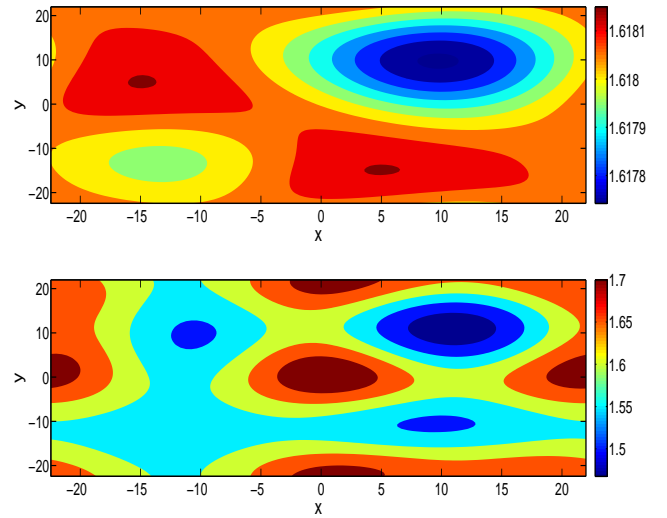


Figure 2: (Color online) Numerical solutions of Eqs. (1) and (2) at $t = 200$ for two different values of r : (a) $r = 1$ and $r = 1.5$ with a fixed $D = 0.1$ and $\chi = 6$. The solutions first increase around the steady-state $(1, 1)$ and then drop to a more or less constant value for a longer time.

first, i.e. $n = 1$ and $k = \pi/L_x = \pi/L_y$. Then, using the condition of instability, for both bounded and unbounded solutions, one may identify a parameter and a critical value below which patterns are regular, while they turn irregular if the parameter is higher than this critical value. If the solution is unbounded, it diverges in a finite time, as shown later. For example, fixing the parameter values $D = 0.1$ and $\chi = 6$, we find that r has a critical value $r_c = 2$, below which the wave pattern is regular or stable, and above which patterns exhibit irregular features. Furthermore, depending on the parameter values considered, there exist a critical value for $k_0 = k/n$, which delimits the range of chaotic pattern formation. The latter also depends on the chemotactic nonlinearity for which the system exhibit finite solutions, as shown in the following subsection.

To obtain steady-state oscillations, we consider the case with $k_0 = 0.07$ (i.e. $n \geq 7$), $D = 0.1$, $\chi = 6$, $k_1 = 0.45 < k < k_2 = 6.9$ and two different values of r : $r = 1$ (upper panel of Fig. 2) and $r = 1.5$ (lower panel of Fig. 2), which fall in the instability region (*c.f.* Fig. 1). Figure 2 shows that initially, the solution lies close to the steady-state value $(1, 1)$ before the organism kinetics dominates. Then, its density or the chemical concentration drops to a steady-state profile determined by the balance between the chemotactic nonlinear term and the dispersive diffusion term. We will later see that the bounded solution may no longer exist and finite-time divergence may develop if the value of r is increased above $r = 2$.

2.1. Variation of the domain length

As the value of k_0 is lowered, i.e. as n increases in order that k falls in the interval (k_1, k_2) , the domain length increases and the regular patterns disappear while irregular spatiotemporal structures arise (see Fig. 3). Basically, the pattern selection leads to

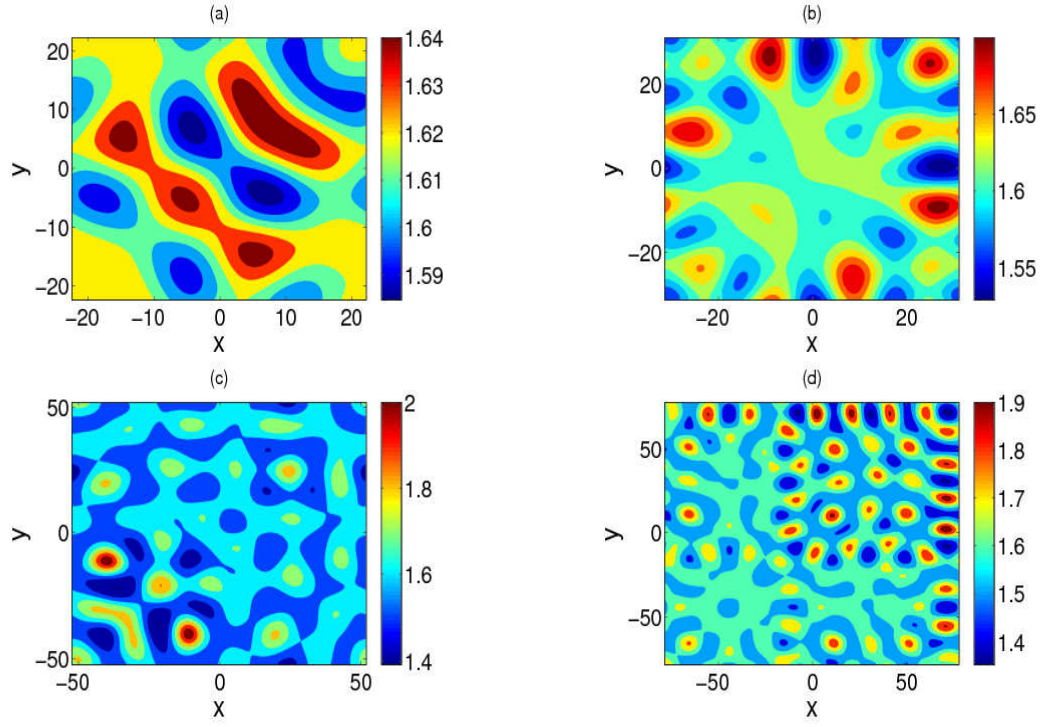


Figure 3: (Color online) Numerical solutions of Eqs. (1) and (2) at $t = 100$. Pattern formation is shown for different domain sizes: (a) $k_0 = 0.07$ (b) $k_0 = 0.05$ (c) $k_0 = 0.03$ and (d) $k_0 = 0.02$. The parameter values are $D = 0.1$, $\chi = 6$ and $r = 2$.

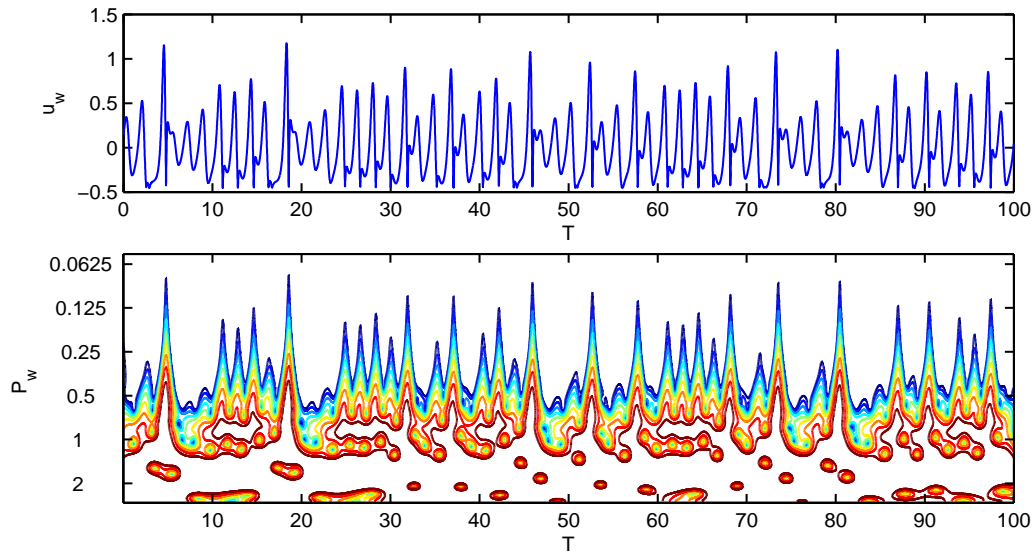


Figure 4: (Color online) Normalized density wave u_w , rescaled by the standard deviation of the sampling data (upper panel) and wavelet power spectra P_w (lower panel) as functions of the sampling time T in logarithmic scale corresponding to Fig. 4(d), indicating chaotic wave trains.

the excitation of many more modes involved in nonlinear interactions. As time advances, collision and fusion of patterns take place, giving rise to higher harmonic modes (merging) and to the emergence of new modes. We also note that increasing the domain size leads to higher concentrations of both u and v at a given time ($t = 100$ in Fig. 3), and enhances the disorder of patterns till a chaotic evolution is established for $r \leq 2$, the condition required for solutions to be bounded. This is illustrated by the analysis of wavelet power spectra portrayed as in Fig. 4.

2.2. Variation of the growth rate

As r exceeds its critical value $r_c = 2$, the solutions quickly evolve and diverge in a finite time (Fig. 5), where the density and the chemical concentration are reported prior to the divergence time. Figure 5 shows four different states at different times, for $D = 0.1$, $\chi = 6$ and $r = 4$. We find that the time of divergence depends on the values of r : smaller r implies longer time before the solution diverges. For instance, the divergence time in Fig. 5 is $t \approx 34$, whereas $D = 0.1$, $\chi = 6$ and $r = 3$ imply a divergence at $t \approx 52$. Further increase of the growth rate r leads to collision and fusion of patterns in a short time when the nonlinear logistic growth term dominates over the diffusion and chemotactic terms. One can calculate the exact divergence times for other sets of parameters.

It is to be noted that since the system is two-dimensional in space, the energy transferred in the nonlinear interactions may not be due to the spatiotemporal chaos as in the previous subsection, but could be primarily related to the wave collapse, i.e., to the divergence of solutions. However, this aspect needs further investigation, which will be subject of future work.

2.3. Combinations of D , χ and r

Next, we explore the pattern dynamics for a set of combinations of the system parameters, especially by increasing the diffusion as well as the chemotactic coefficient. Both parameters control various distinctive features. Comparing the upper panel of Fig. 6 with Fig. 3(d), we note that increasing χ stabilizes oscillations by reducing the values of u and v . On the other hand, increasing the diffusion coefficient, while keeping the other parameters fixed as in Fig. 3(d), one can observe chaotic patterns similar to those of Fig. 3(d) (*c.f.* lower panel of Fig. 6). This can be explained as follows. As χ increases, with D and r fixed, the region of instability determined by the values of k increases, since its lower limit k_1 decreases while its upper limit k_2 increases. In other words, n may be smaller or fewer modes may be involved in the nonlinear dynamics leading to chaos. On the other hand, when D increases with other parameters fixed, the instability region is strongly reduced, since the opposite happens with the lower limit and upper limits for k , and n has to be larger in order for k to fall within the instability region $k_1 < k < k_2$. Thus, many more modes will participate in the collision and fusion process, and as a result spatiotemporal chaotic patterns may likely arise. Figure 7 represents the contour plot of the wavelet power spectra, corresponding to Fig. 6, plotted against a normalized sampling time T (lower panel). This shows that the system is chaotic for a long time interval.

It is also interesting to observe that the dynamics become more complex in nature at large values of t [*c.f.* Fig. 7(d)].

3. Conclusions

We have explored the nonlinear dynamics of a (2+1)-dimensional chemotaxis model of KS-type. Specifically, by numerical simulations, we have focused on the existence of bounded solutions, solutions which diverge in finite-time as well as on the formation of different patterns including those arising from merging.

In the parameter range, where the solutions remain permanently bounded, the existence of spatiotemporal chaotic states is demonstrated by the analysis of wavelet power spectra. These phenomena are important in the context of chemotactic migration but so far, to the best of our knowledge, have not been explored in two-dimensional KS models. We have shown that an increase of the chemotactic coefficient ($\lesssim 10$) and/ or keeping the growth rate ($r \leq 2$), stable solutions around the steady-state are generated after a long time ($t \gtrsim 200$). Furthermore, taking the growth rate beyond its critical value leads to the finite time divergence of the solutions for the density and the chemical concentration. Concerning pattern formation and evolution in a large domain, suitable combinations of the parameters χ , D and r , e.g. $5 \lesssim \chi \lesssim 10$ and $1 < r \lesssim 2$, lead to bounded solutions which develop spatiotemporal chaos, whose complexity grows in time.

Acknowledgement

A.P.M. acknowledges support from the Kempe Foundations, Sweden.

References

- [1] E.F. Keller, L.A. Segel, *J. Theor. Biol.* 26 (1970) 399.
- [2] P. Biler, *Adv. Math. Sci. Appl.* 9 (1999) 347.
- [3] P. Biler, T. Nadzieja, *Colloq. Math.* 66 (1993) 131.
- [4] P. Biler, T. Nadzieja, *Report. Math. Phys.* 52 (2003) 205.
- [5] T. Hillen, K. J. Painter, *J. Math. Biol.* 58 (2009) 183.
- [6] K.J. Painter, T. Hillen, *Physica D* 240 (2011) 363.
- [7] Z. Wang, T. Hillen, *Chaos* 17 (2007) 037108.
- [8] M.P. Brenner, L. Levitov, E.O. Budrene, *Biophys. J.* 74 (1995) 1677.
- [9] M.D. Betterton, M.P. Brenner, *Phys. Rev. E* 64 (2001) 061904.
- [10] J. Song, D. Kim, *Phys. Rev. E* 58 (2009) 183.
- [11] Z.A. Wang, *Math. Model. Nat. Phenom.* 5 (2010) 173.
- [12] Y.S. Choi, Z.A. Wang, *J. Math. Anal. Appl.* 362 (2010) 553.
- [13] H.C. Berg, D.A. Brown, *Nature (London)* 239 (1972) 500.
- [14] J. Adler, *Science* 166 (1969) 1588.
- [15] S.S. Willard, P.N. Devreotes, *Eurro. J. Cell. Biol.* 85 (2006) 897.
- [16] W. Alt, *J. Math. Biol.* 9 (1980) 147.
- [17] H.G. Othmer, A. Stevens, *SIAM J. Appl. Math.* 57 (1997) 1044.
- [18] A. Stevens, *SIAM J. Appl. Math.* 61 (2000) 183.

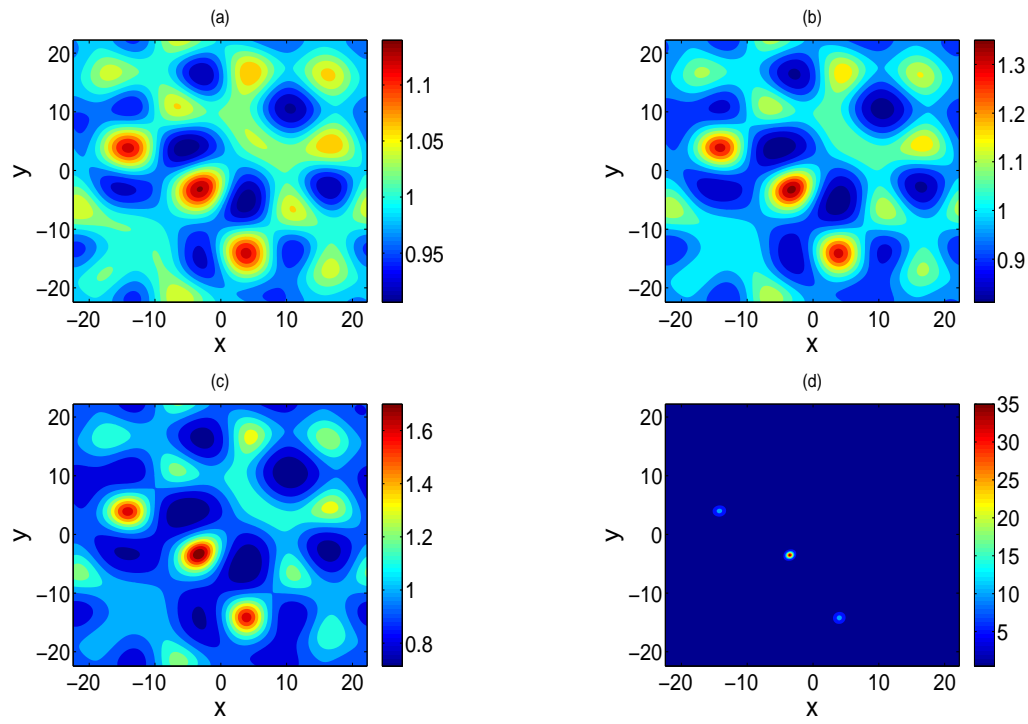


Figure 5: (Color online) Numerical solutions of Eqs. (1) and (2). Pattern formation and solutions diverging in a finite time are shown at different times before divergence: (a) $t = 25$, (b) $t = 28$, (c) $t = 30$ and (d) $t = 34$. The parameter values are $D = 0.1$, $\chi = 6$ and $r = 4$.

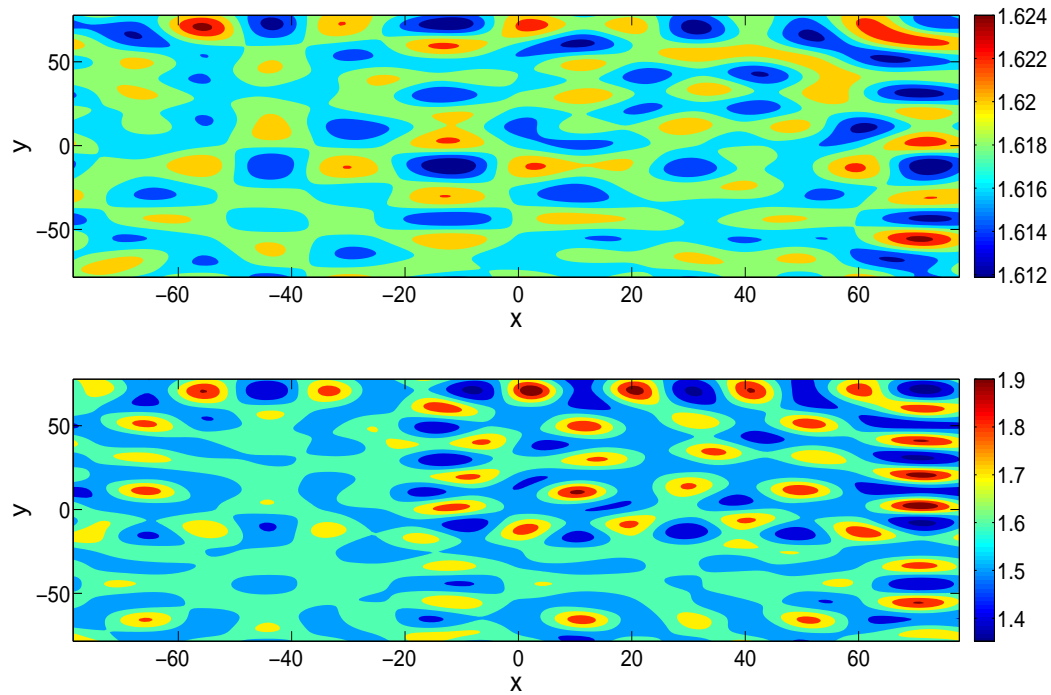


Figure 6: (Color online) Pattern evolutions as solutions of Eqs. (1) and (2) for different combination of parameters: (a) $D = 0.1$, $\chi = 10$ and $r = 2$ at $t = 100$, (b) $D = 1$, $\chi = 6$ and $r = 2$ at $t = 100$.

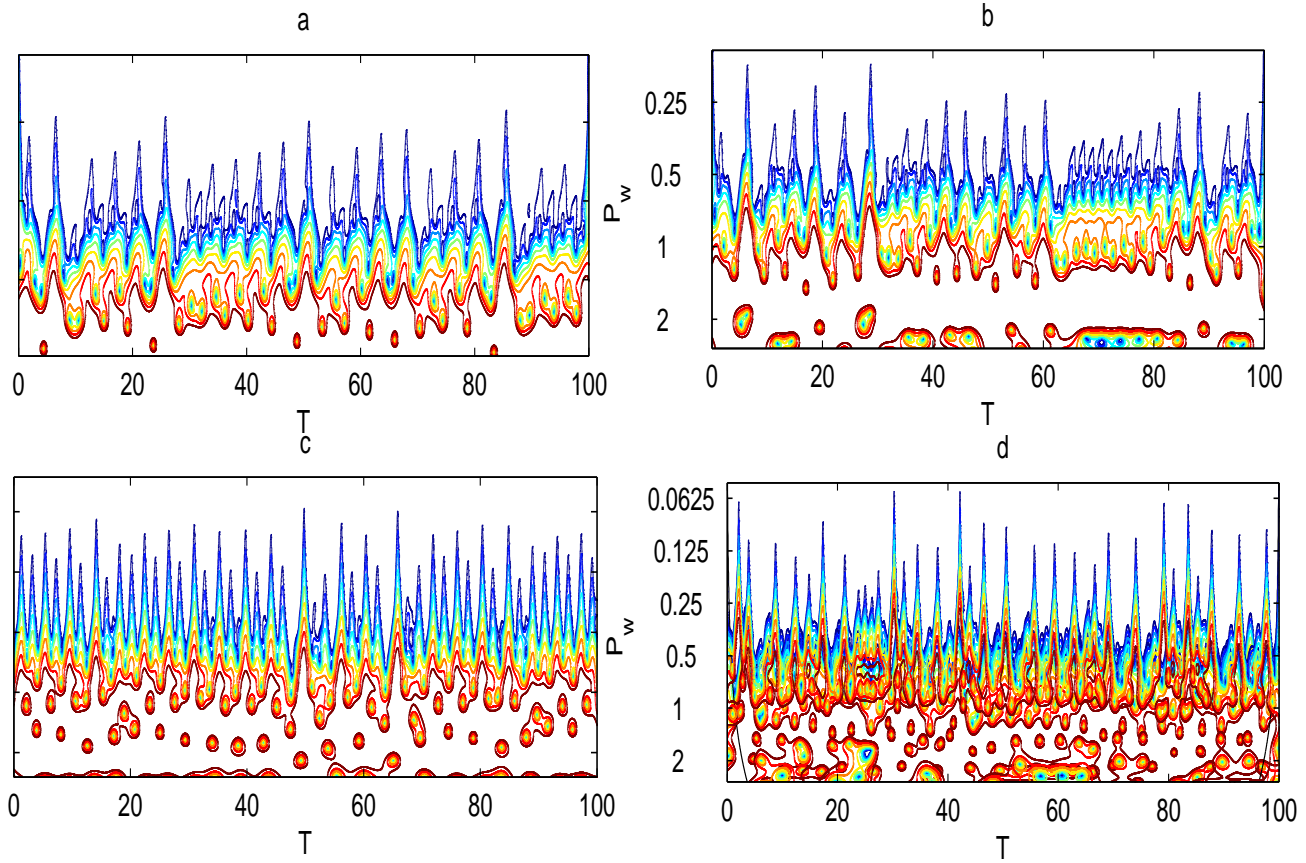


Figure 7: (Color online) Contour plot of the wavelet power spectra corresponding to Fig. 6 (lower panel) for (a) $t=100$, (b) $t=500$, (c) $t=1000$, (d) $t=5000$.